Solid-State NMR and Density Functional Investigation of Carbon-13 Shielding Tensors in Metal−Olefin Complexes†

Robert Havlin,¶ Michael McMahon,‡ Ranjani Srinivasan, Hongbiao Le,# and Eric Oldfield*

Department of Chemistry, University of Illinois at Urbana−Champaign, 600 South Mathews Avenue, Urbana, Illinois 61801

Received: June 24, 1997⊗

We have determined the principal elements of the chemical shift tensors for a series of metal−olefin complexes: $[Ag(cod)_2]BF_4$ (cod = *cis*,*cis*-cycloocta-1,5-diene), $[CuCl(cod)]_2$, $PtCl_2(cod)$, $[RhCl(cod)]_2$, and $K[PtCl_3(C_2H_4)]$ using magic-angle sample spinning and a Bayesian probability method to deduce μ, ρ in the Herzfeld-Berger equations. These principal elements have also been computed by using density functional methods with two different types of functionals and partial geometry optimization. The overall slope and R^2 values between the theoretical and experimental tensor elements are good, ranging from 1.06 to 1.16 for the slope (versus the ideal value of 1) and 0.98−0.99 for the goodness of fit parameter R^2 (versus the ideal value of 1). The use of a hybrid functional results in a slightly worse slope, an effect which is largest for the compounds with the largest paramagnetic shifts. There are no particularly good correlations between C−C bond lengths, isotropic/anisotropic shift tensor elements or computed bond orders; however, the correlation between shielding and (Mulliken) charge of ~ -120 ppm/electron is consistent with previous experimental estimates on olefins and aromatic compounds. The orientations of the shielding tensor elements in the cod complexes change in a relatively continuous manner with increases in shielding (from d^{10} to d^8 metals), with δ_{33} becoming rotated (37.5°) from the normal to the C═C bond axis in $[RhCl(cod)]_2$. Overall, these results indicate that density functional methods permit the relatively accurate reproduction of metal−ligand shielding patterns in systems whose structures are known, which should facilitate their use in probing metal−ligand geometries in systems whose structures are less certain, such as in metalloproteins.

Introduction

Nuclear magnetic resonance (NMR) spectroscopy has become one of the more powerful methods for probing molecular structure in solution.[1] However, it has only been in the past few years that theoretical methods have enabled the successful reproduction of one of the more important NMR spectroscopic observables, the chemical shift, in large molecules.[2] Here, major advances by Ditchfield,[3] Wolinski et al.,[4] Schindler and Kutzelnigg et al.,[5] Malkin et al.,[6] Schreckenbach and Ziegler,[7] and Frisch et al.[8] have enabled the successful prediction of many isotropic shifts in organic and bioorganic systems—even including molecules as large as proteins.[9] One of the goals of our research is to be able to use such quantum chemical methods, combined with solid-state NMR, to enable the investigation of metal−ligand interactions, as well as the metal centers themselves, in metalloproteins. To date, however, there have been relatively few studies made of metal or ligand shielding tensors using solid-state NMR and quantum chemistry. In earlier work[10] we reported the ^{13}C and ^{17}O shift tensors for CO bonded to Cr, Mo, and *W*, and more recently, Kaupp et al.[11] and Schreckenbach and Ziegler[7] have analyzed these results by using density functional theory (DFT). DFT methods appear to handle in a very effective way the effects of electron correlation and exchange and have enabled the accurate prediction and analysis of CO shielding tensor information. These systems are of interest since they contain both ligand → metal donation and metal → ligand back-donation contributions to bonding, which influence shielding.

A second important class of compounds containing simultaneous ligand σ-donation and metal π-back-donation are olefin containing metal complexes. Solid-state NMR spectra of olefins[12,13] and their complexes[14] have been obtained by several workers over the years, but until recently it would have been a very challenging proposition to accurately predict the shielding tensors for these metal−ligand complexes, even though the basic aspects of metal−ligand bonding in olefin complexes have been studied for many years.[15−17] Our goal here, therefore, is first to obtain accurate shielding tensor information for olefin ligands in a series of metal−olefin complexes, and second, to use density functional methods to predict the magnitudes, as well as the orientations, of the principal elements of the ^{13}C shielding tensors of the olefin carbons when bonded to metals such as Ag, Cu, Pt, and Rh. In addition, we chose to investigate ^{13}C shielding in a Fisher carbene as a further test of the predictive ability of current theoretical methods.

In this paper, we focus on the acquisition and/or the prediction of the solid-state ^{13}C NMR chemical shieldings of six organometallic compounds: $[RhCl(cod)]_2$, $PtCl_2(cod)$, $K[PtCl_3(C_2H_4)]$, $[CuCl(cod)]_2$, $[Ag(cod)_2]BF_4$, and $(CO)_5Cr{=}C(CH_3)(OEt)$ (cod = cis,cis-cycloocta-1,5-diene). We use density functional methods and investigate the use of two different functionals. In cases where H atom coordinates were unavailable or poorly defined, we have used ab initio quantum chemical geometry optimization methods to predict their positions. The overall shielding results are good, especially for the simple olefin complexes, with correlation coefficients between theory and experiment of ≥ 0.98 being obtained for the olefinic carbons, and there are seen to be only relatively minor changes in the

† This work was supported by the United States Public Health Service (National Institutes of Health Grant HL-19481).

¶ Barry Goldwater Fellow.

‡ National Institutes of Health Cellular and Molecular Biophysics Training Grant Trainee (Grant GM-08276).

Present Address: Laboratorium für Physikalische Chemie, ETH Zürich, Switzerland.

⊗ Abstract published in *Advance ACS Abstracts,* September 15, 1997.

S1089-5639(97)02058-6 CCC: $14.00

orientations of the tensors on metal bonding, which is consistent with the qualitative ideas put forth by Wallraff.[14]

Experimental Section

Synthetic Aspects. $[CuCl(cod)]_2$ was prepared by allowing SO_2 to diffuse into a solution of $CuCl_2 \cdot 2H_2O$ and cod in ethanol at 0 °C.[18] $[Ag(cod)_2]BF_4$ was synthesized by adding cod to a suspension of $AgBF_4$, under nitrogen, at −10 °C.[19] $[RhCl(cod)]_2$, $PtCl_2(cod)$ and Zeise's salt ($K[PtCl_3(C_2H_4)]$) were purchased from the Sigma-Aldrich Chemical Co. (St. Louis, MO).

Nuclear Magnetic Resonance Spectroscopy. ^{13}C NMR spectra were obtained on two "home-built" 11.7 T (500 MHz ^1H resonance frequency) spectrometers equipped with "magic-angle" spinning (MAS) probes from Doty Scientific (Columbia, SC). Spinning speeds ranged from 2 to 5 kHz. Highly accurate and precise spinning speeds were obtained by the use of a Doty Scientific spin speed controller. Spectra were obtained with use of cross polarization under conditions of high-power proton decoupling. Mix times ranged from 0.75 to 2.5 ms. All of the spectra were obtained using a recycle time of 7 s.

Computational Aspects. Shielding calculations were carried out on a cluster of RISC workstations (International Business Machines, Austin, TX), RS/6000 Models 340, 350, 360, 365, and 3CT. We employed two approaches. In the first, we used the coupled sum-over-states/density functional theory/individual gauges for localized orbitals (SOS/DFT/IGLO) approach of Malkin, Salahub et al.,[6] while in the second we used the uncoupled density functional/gauge including atomic orbitals (DFT/GIAO) approach as implemented in Gaussian 94.[8] In the SOS-DFPT method we used a Perdew−Wang (PW91) functional and a fine integration grid. The carbon atoms of interest were represented by an iglo-iii[20] basis set, while other light elements were represented by iglo-ii basis sets. For the metals, we used an all electron representation[21] except for rhodium and platinum, where effective or model core potentials (ECPs or MCPs) were employed.[21] A second set of calculations were carried out in Gaussian 94 using this time a hybrid functional, Becke's three-parameter functional, combined with the Lee, Yang, and Parr correlation functional (B3LYP).[22] The basis for the carbons of interest was 6-311++G(2d,2p), while LanL2DZ ECPs[23] were used on the metals. The NMR shielding tensors were calculated using the gauge-including atomic orbital (GIAO) method.[3]

Atomic coordinates were taken from previously determined X-ray structures.[19,24−26] In cases where hydrogen atom coordinates were unavailable, hydrogen atoms were added, and the structures geometry optimized with respect to the hydrogen atom positions only, using the BPW91 functional in Gaussian 94, with a 6-31G* basis on nonmetal atoms and LanL2DZ ECPs on the metals.

Results and Discussion

We show in Figure 1 the ^{13}C MAS NMR spectra of $[CuCl(cod)]_2$

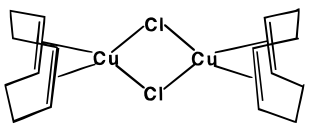

at spinning speeds of 2.5 and 4.0 kHz ± 5 Hz. As may be seen from Figure 1, crystallographic packing causes a small (∼10 ppm) chemical shift nonequivalence for the center band (on average at 118.8 ppm downfield from TMS) and its

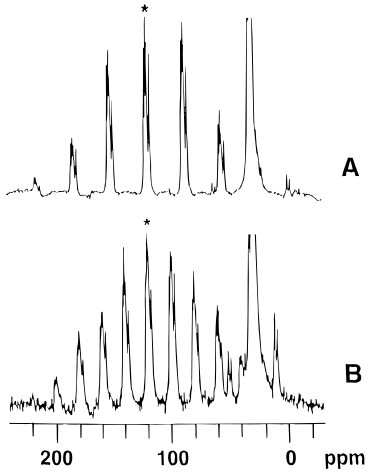

Figure 1. 11.7 T cross-polarization proton-decoupled magic-angle sample-spinning carbon-13 Fourier transform NMR spectra of $[CuCl(cod)]_2$ at 300 K: A, spin speed = 4000 ± 5 Hz; B, spin-speed = 2500 ± 5 Hz.

associated spinning sidebands. When such nonequivalences were observed, we simply report average shift values, to be compared with average shielding values from the DFT calculations, since it is not at present possible to make specific, crystallographically related peak assignments. The intensities of the centerbands and spinning sidebands were then used to deduce the principal components of the ^{13}C shift tensors using a somewhat modified version of the Herzfeld−Berger (HB) method[27] which we find to be quite robust, since it enables accurate tensor determinations in difficult situations (missing centerbands, low signal-to-noise (S/N) ratios, close to axial symmetry) and is now used routinely in our laboratory.

The principal elements of the shielding tensor are related to the parameters μ and ρ in the HB method in the following manner:

$$\mu = (\gamma H_0)(\sigma_{33} - \sigma_{11})/\omega_r \quad (1)$$

$$\rho = (\sigma_{11} + \sigma_{33} - 2\sigma_{22})/(\sigma_{33} - \sigma_{11}) \quad (2)$$

The relative intensity of a given sideband can be evaluated for a particular spinning speed if the elements of the tensor are known. In our approach, we use a Bayesian probability method in which the probability Z that an experimentally determined sideband intensity, I_{expt}, given by a particular μ, ρ pair, is

$$Z = \exp[-(I_{expt} - I^{calc}_{\mu,\rho})^2/W^2] \quad (3)$$

where $I^{calc}_{\mu,\rho}$ is a matrix element representing the μ, ρ surface specific to the sideband number, and W is a variable search width parameter. The $I_{\mu,\rho}$ matrix was calculated from the integrals described,[27] which are available on request for n = 1−20. For any two sideband intensities, there is as expected a wide range of μ, ρ values that give the anticipated sideband intensities, as shown in Figures 2A,B. However, the probability surfaces for different sidebands can be multiplied, and as shown in Figure 2C the allowed μ, ρ values rapidly decrease. Figure 2D shows a result for a ^5Z surface (five sideband intensities), with the highest probability contour yielding μ = 5.4 and ρ = 0.17. From such multiple Z surfaces, the parameters μ and ρ were determined from the highest probability values, typically greater than 0.95 for the nth root of Z, where n is the total number of sidebands employed. The isotropic chemical shifts were then combined with the parameters μ and ρ to determine the three principal components of the chemical shielding tensor.

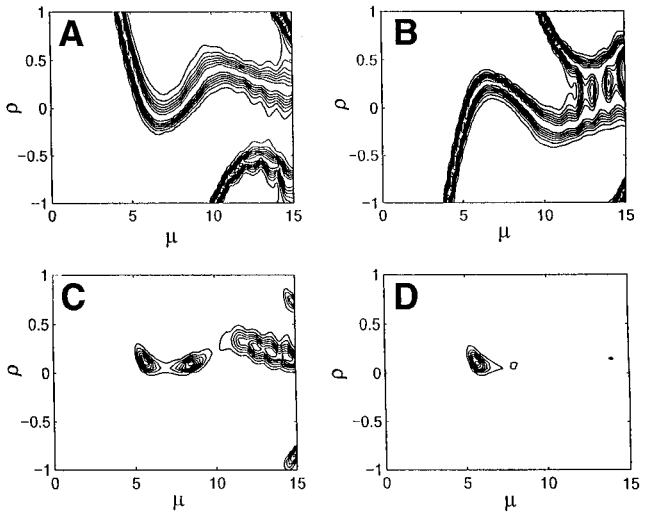

Figure 2. Bayesian probability μ, ρ surfaces for evaluation of shielding tensor elements for $[CuCl(cod)]_2$. Experimental intensity data taken from Figure 1: A, ^2Z, sidebands 0 and +1; B, ^2Z, sidebands 0 and −1; C, ^3Z, sidebands 0 and ±1; D, ^5Z, sidebands 0, ±1, and ±2 were used.

In instances where there was additional chemical shift nonequivalence (due to crystallographic effects, as in Figure 1), we used the entire unresolved sideband intensity, since it is not at present possible to make site-specific assignments. The experimental isotropic shifts are reported in Table 1, together with additional solid-state results on cod, C_2H_4, and a Fischer carbene.[14]

We then calculated the isotropic chemical shieldings and the principal components of the chemical shielding tensors, using the deMon SOS/DFPT/IGLO method. The agreement between experimental shift and calculated shielding values is very good, with a slope of −1.10 and an R^2 value of 0.967 for the isotropic shifts (Figure 3A), and a slope of −1.06 and an R^2 value of 0.981 for the tensor elements (Figure 3B). We also present these results in Table 1 in terms of the computed chemical shifts, where for convenience we have converted the calculated shieldings (σ, ppm from the bare nucleus, Figures 3A,B) to calculated shifts, using the conversion factor of 186.5 ppm for the absolute shielding of TMS.[28] This value is in fortuitously good accord with the shielding intercept of 186.6 ppm obtained from the shielding calculation results shown in Figure 3. Clearly though, there is very good agreement between the theoretical and experimental shift results, both in terms of the isotropic shifts, the anisotropic shieldings, as well as the absolute shieldings observed in each of the olefin and metal−olefin systems investigated (Table 1). For the Fischer carbene, $(CO)_5Cr{=}C(CH_3)(OEt)$, there is respectable agreement, although the overall width of the tensor is underestimated. This is unlikely to be due solely to an error in the experimental (NMR and X-ray) measurements, since as we see below somewhat different results are obtained when using a different calculational approach. With the exception of the Fischer carbene, then, all other results are very good. The largest error occurs with the most deshielded tensor element in $[Ag(cod)_2]BF_4$, an effect which could be due to the difficulties associated with handling charge field effects in the crystal lattice, but the error is small. In additional studies using an iglo-ii basis on all light atoms, we found very little change in the correlation between theory and experiment, although the absolute shielding intercept degraded to 192.9 ppm, versus the ideal value of 186.5 ppm. The slope also changed to 1.03, with an R^2 value of 0.983.

We next calculated each of the shielding tensor elements using a somewhat different approach, the uncoupled DFT/GIAO method available in Gaussian 94. We carried out these additional calculations to explore the effects of using hybrid functionals, which are of particular use in calculating properties of transition metal ions such as chemical shifts[29,30] and electric field gradients,[31] since we anticipated the need to use hybrid functionals when probing metal−ligand interactions in metalloproteins, where both metal and ligand properties might be required. Of course, there are not only differences in functionals in this case, but also differences in basis sets, as well as different approaches to handing the gauge question, and the use of coupled vs uncoupled approaches—but as we show below the main conclusion of this second set of calculations is that both approaches yield very good accord between experiment and prediction.

We show in Table 1 and Figure 4 the ligand shift and shielding results obtained. The B3LYP functional displays the same small scatter observed in the deMon calculations, with an R^2 value of 0.99 for the tensor elements and 0.962 for the isotropic shifts (versus 0.981 and 0.967 for deMon). In both cases the slope degrades somewhat, from −1.10 to −1.18 for the isotropic shifts (σ_i) and −1.06 to −1.161 for the tensor elements (σ_{ii}) (Figures 4A,B). The RMSD values versus the correlation line are 4.0 ppm (σ_i) and 10.3 ppm (σ_{ii}) for the deMon SOS/DFPT/IGLO approach, and 5.8 (σ_i) and 8.3 ppm (σ_{ii}) for the B3LYP/GIAO Gaussian 94 method, with the error on the tensor elements being at the level of experimental uncertainty.

Interestingly, the deviations from the straight line are not particularly well correlated between the two calculations. A very high correlation might reasonably be expected to be seen if the errors were in the shielding tensor elements or in the crystallographic structures, since these errors would be common. It is possible that charge field effects, relativistic effects in the calculations and in the geometry optimization might all be important, although the errors seen could easily have a major contribution due solely to experimental uncertainty. For the Fischer carbene, neither calculation gives particularly good accord with the experimental results, Table 1, although the error appears largest with the calculation using the B3LYP functional. Although we have not investigated the functional dependence of shielding in detail, it does appear that ligand shieldings may be overestimated somewhat with B3LYP, an effect which has been noted for ^{15}N and ^{17}O shifts previously by others.[32,33]

Next, we consider the actual orientations of the shielding tensors. In previous work, Wallraff postulated that the tensor elements would not change significantly on metal bonding,[14] essentially because the d^8 and d^{10} transition metal complexes are not particularly metallacyclopropane-like. For example, the ^{13}C shielding tensor in cyclopropane itself is quite unlike that seen in the olefin complexes, having a breadth of only ∼60 ppm. We show in Figure 5 the orientations of the ^{13}C shielding tensor in the four metal−cod complexes. The most shielded element σ_{33} is approximately perpendicular to the olefinic plane, and changes in magnitude relatively little with metal substitution, since there are only minor olefin in-plane bonding changes. However, both σ_{11} and σ_{22} do change in magnitude considerably on metal complexation, due to a combination of σ-donation and π-back-donation effects, with σ_{11} and σ_{22} being perpendicular to the metal−olefin bond axis. For the orientational changes, we define two angles α and β to compare the changes in tensor orientation among the different compounds. Here, α is the angle between σ_{33} and the olefinic C−C bond axis, and β is the angle that σ_{22} makes with the olefinic C−C bond axis. The results of Table 2 show that there is a general correlation of α and β with isotropic shift for $[Ag(cod)_2]BF_4$, $[CuCl(cod)]_2$, Pt Cl_2-(cod) and $[Rh(cod)]_2$, indicating a gradual tilting of the tensor

TABLE 1: Experimental and Theoretical ^{13}C Shifts and Shift Tensor Elements for Metal−Olefin Complexes

	chemical shifts, ppm[a]														
	experimental					SOS/DFPT (calcd)					G94/B3LYP (calcd)				
system	δ_{iso}	δ_{11}	δ_{22}	δ_{33}	Ω^b	δ_{iso}	δ_{11}	δ_{22}	δ_{33}	Ω^b	δ_{iso}	δ_{11}	δ_{22}	δ_{33}	Ω^b
cod[c]	128.0	238.0	126.0	21.0	217.0	141.5	257.3	131.4	35.8	221.5	137.6	260.0	124.0	28.8	231.2
C_2H_4[d]	126.0	234.0	120.0	24.0	210.0	125.1	239.3	121.6	14.5	224.8	126.1	250.4	115.4	12.6	237.8
$[Ag(cod)_2]BF_4$	124.8	225.0	115.0	34.0	191.0	135.6	253.1	124.1	29.7	223.4	131.0	253.4	119.8	19.9	233.5
$[CuCl(cod)]_2$	118.8	203.5	116.0	36.5	167.0	125.1	221.2	121.8	32.8	187.6	123.6	227.0	121.4	22.4	204.6
$PtCl_2(cod)$	103.0	182.3	104.0	18.0	164.3	107.5	171.0	125.5	26.0	145.0	93.3	188.1	94.6	−2.8	190.9
$[RhCl(cod)]_2$	80.5	161.7	76.7	20.5	141.2	91.2	179.5	73.5	21.9	158.3	78.6	167.7	66.3	1.8	165.9
$K[PtCl_3(C_2H_4)]$	75.9	160.0	68.0	0.0	160.0	74.4	152.3	63.9	8.6	143.7	72.2	154.7	59.3	2.6	152.1
$(CO)_5Cr{=}C(CH_3)(OEt)$[e]	301.3	675.0	186.0	43.0	632.0	337.5	660.0	236.5	116.1	543.9	387.1	805.0	248.7	107.6	697.4

[a] Converted from absolute shielding values using $\delta = 186-\sigma$. [b] Chemical shift anisotropy breadth $\Omega = \delta_{11}-\delta_{33}$. [c] Reference 36. [d] Reference 12. [e] Reference 14.

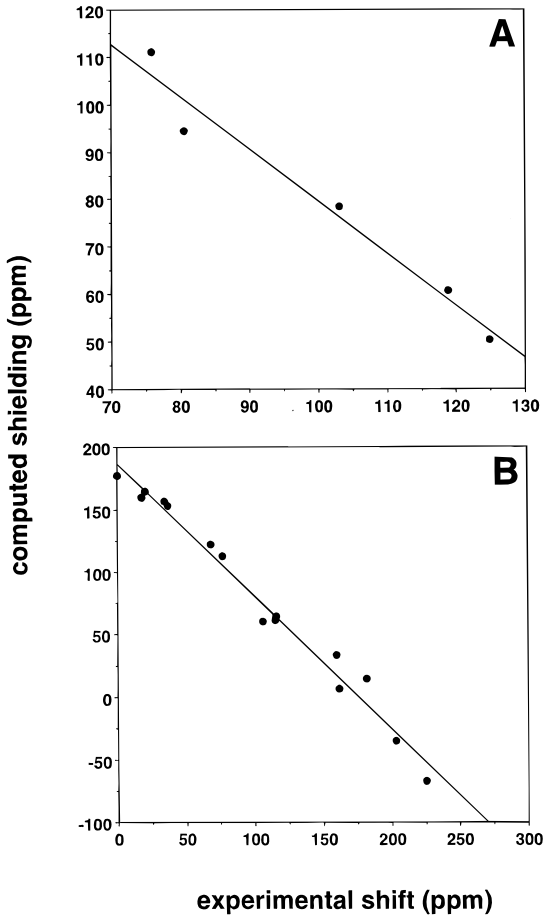

Figure 3. Graphs showing experimental versus theoretical isotropic shieldings and individual shielding tensor element correlations for $[Ag(cod)_2]BF_4$, $[CuCl(cod)]_2$, $PtCl_2(cod)$, $[RhCl(cod)]_2$, and $K[PtCl_3(C_2H_4)]$, evaluated as described in the text using the deMon program. A, isotropic shifts/shielding: slope = −1.10, R^2 value = 0.967. B, anisotropic shifts/shielding tensor components: slope = −1.06, R^2 value = 0.981.

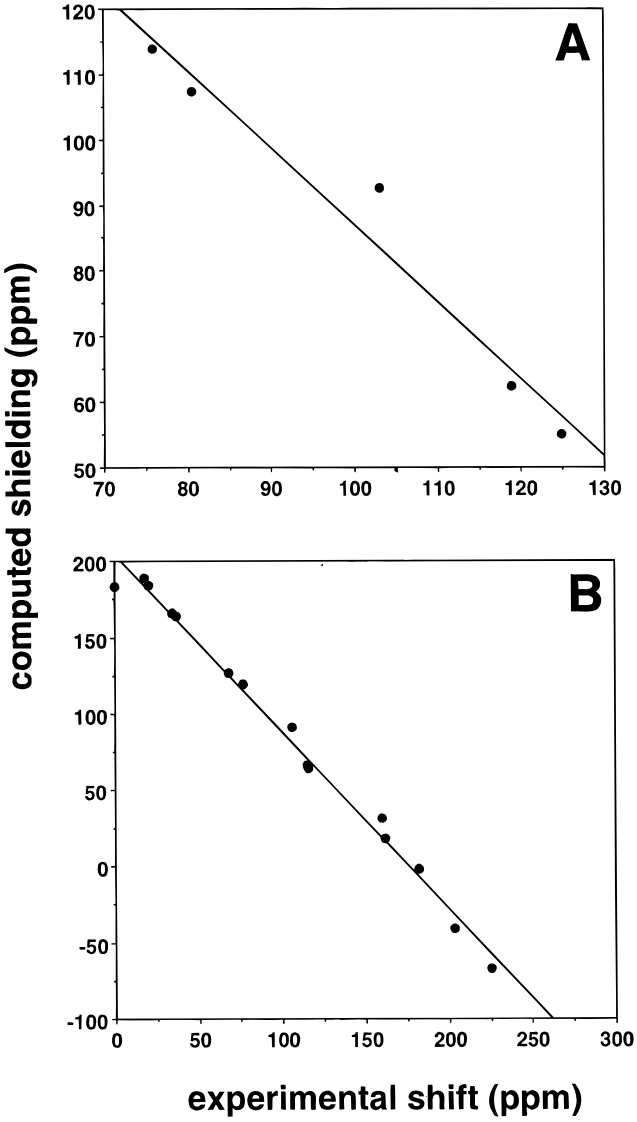

Figure 4. Graph showing experimental versus theoretical shifts/shieldings computed using Gaussian 94/B3LYP hybrid functional, as described in the text. Compounds studied as in Figure 3. A, isotropic shifts/shielding: slope = −1.18, R^2 value = 0.962. B, anisotropic shifts/shielding tensor components: slope = −1.16, R^2 value = 0.99.

with increased back-bonding/shielding, in addition to the major changes in the magnitude of σ_{11} and σ_{22} shown in Table 1. The result for Ziese's salt falls off of this trend, presumably due to the lack of alkyl substituents on the olefin.

Finally, with this body of both experimental and theoretical shielding tensor results at hand, we searched for possible correlations between structure and shielding or between shielding and another derived parameter. We found no striking correlations between olefin bond length/isotropic shift, olefin bond length/shielding tensor element, Mayer bond order/isotropic chemical shift, Mayer bond order/shielding tensor element, Mulliken population (charge)/isotropic shift, or Mulliken population/anisotropic shielding tensor element. In essentially all cases, trends could be discerned, but they would not be useful to establish, e.g., a bond length, with precision.

There are some trends observed, which are, however, of interest. For example, we find that a correlation between Mulliken population (net charge) on carbon and the actual magnitudes of the tensor elements exists. For the most shielded component σ_{33}, the slope is 95 ppm/e$^-$ ($R^2 = 0.84$), for σ_{22} the

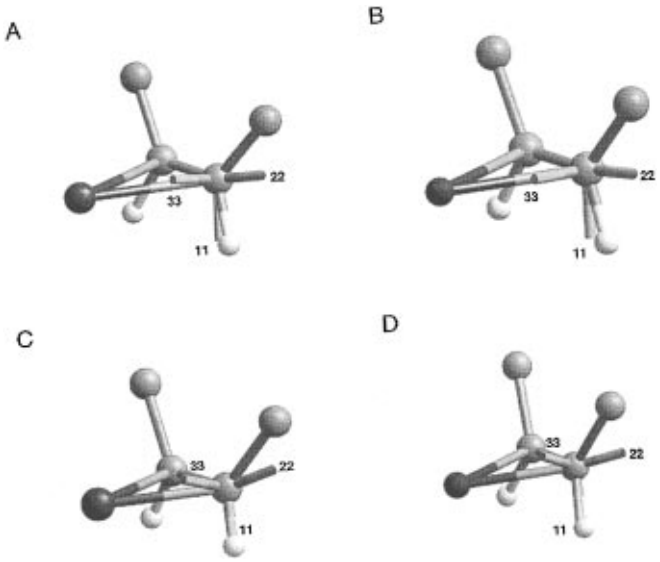

Figure 5. Orientations of the olefinic shielding tensors in the four cod complexes investigated. A, $[Ag(cod)_2]BF_4$; B, $[CuCl(cod)]_2$; C, $PtCl_2(cod)$; and D, $[RhCl(cod)]_2$. The large dark sphere to the left of each structure is the heavy metal; the small light spheres are the hydrogen atoms.

TABLE 2: Orientation of Tensor Elements

system	α^a	β^b
C_2H_4	90	0
$BF_4[Ag(cod)_2]$	90.5	16.6
$[CuCl(cod)]_2$	90.8	12.1
$PtCl_2(cod)$	93.9	28.2
$[RhCl(cod)]_2$	107.3	37.5
$K[PtCl_3(C_2H_4)]$	101.8	11.8

[a] α is the angle that δ_{33} makes with respect to the olefinic C−C bond. [b] β is the angle that δ_{22} makes with respect to the olefinic C−C bond axis.

TABLE 3: Computed Mayer Bond Orders

system	bond order[a]
cod	1.96
C_2H_4	1.99
$BF_4[Ag(cod)_2]$	1.54
$[CuCl(cod)]_2$	1.56
$PtCl_2(cod)$	1.12
$[RhCl(cod)]_2$	1.34
$K[PtCl_3(C_2H_4)]$	1.27

[a] Average order of carbon−carbon double bonds.

result is 134 ppm/e$^-$ ($R^2 = 0.69$), while for σ_{11} the R^2 value is very poor ($R^2 = 0.39$) and the slope is 124 ppm/e$^-$. There are nevertheless two interesting features: first, the general pattern seen experimentally, the changes in σ_{11} and σ_{22} are greater than those seen with σ_{33}, is apparent. Second, the changes in the individual tensor elements with added charge, 124, 134, and 95 ppm/e$^-$, give an average value of 118 ppm/e$^-$ for the isotropic shift. This is similar to the experimentally deduced value of ~160 ppm/e$^-$, deduced many years ago, on the basis of chemical shift measurements of charged and neutral compounds.[34]

Another trend of interest is the observation that, while the computed C−C Mayer bond orders clearly cluster (Table 3), they are only weakly related to shielding. For example, the ethylene and cod bond orders are 1.96 and 1.99, while those in the d^{10} Ag^I and Cu^I complexes are only 1.54 and 1.56, a large difference in bond order, but certainly in the case of Ag, only a minor change in shielding (Table 1). For the d^8 complexes of Pt and Rh, the bond orders decrease to 1.12 and 1.34, and there is a major increase in shielding, but the overall correlation between bond order and shielding is poor ($R^2 = 0.384$), due to the anomalously low bond order in the $PtCl_2(cod)$ complex (Table 3).

We should also note here that quantum chemical methods are also of use in testing other ideas about the various contributions to shielding. For example, in the case of Zeise's salt, it is well-known[35] that there is a bend-back of the olefinic protons, forming a more nearly tetrahedral carbon. The direct effect of this distortion on shielding is, however, only small. Calculations show that for the shift from a planar to a distorted geometry there is only a 12 ppm increase in isotropic shielding. However, the effects of lengthening the C−C bond, from 1.34 to 1.44 Å, as observed for example in ethylene in Zeise's salt, results—in ethylene itself—in a 20 ppm increase in shielding, so about $^2/_3$ of the total shielding effect seen on going from ethylene to C_2H_4 in Zeise's salt can in fact be attributed to geometric changes.

Conclusions

The results presented above represent the first theoretical predictions of the ^{13}C shifts and shielding tensor elements for a series of metal−olefin complexes. There is very good accord between theory and experiment for both the isotropic shifts as well as the individual shielding tensor elements using two different density functional approaches, with both methods giving R^2 values of >0.98 and good slopes. The most shielded tensor element σ_{33} is oriented approximately perpendicular to the olefin plane (along the M−C_2 bisector), σ_{22} is approximately along the C−C bond axis, while the least shielded tensor element σ_{11} is in the olefin plane. The two components perpendicular to the metal−olefin axis (σ_{11} and σ_{22}) are, as expected, most susceptible to changes in metal−ligand bonding (change in metal and number of d electrons). On increasing back-bonding/shielding, the tensor rotates, with δ_{33} moving up to 37.5° away from perpendicular. For the Fischer carbene, $(CO)_5Cr{=}C(CH_3)(OEt)$, the carbene tensor is moderately well predicted using the coupled Malkin−Salahub SOS/DFPT method, but rather less well so with the uncoupled G94/GIAO/B3LYP approach, an effect which may be general in systems with very low-lying excited states. For both sets of calculations, there are no dramatic correlations between the spectroscopic observables and bond lengths or bond orders, although a correlation between net charge on carbon and shift is seen, and geometric distortions are shown to make a direct and nonnegligible contribution to shielding in the case of Zeise's salt.

Overall, the ability to quite accurately predict both isotropic shifts and shielding tensor elements in a wide range of metal−olefin complexes gives additional confidence in the combined use of NMR and DFT methods as probes of molecular structure in materials whose structures are less well defined than those investigated herein, such as in metalloenzymes and metalloproteins, where (isoelectronic) O_2 and RNO as well as CO and RNC ligands are all known to bind tightly to metals. In particular, the ability to rather accurately compute individual tensor elements from known or suspected structures should place strong restraints on what structures are in fact possible.

Acknowledgment. We thank Professor D. Salahub and Drs. V. Malkin, O. Malkina, and E. Proynov for providing their deMon program.

References and Notes

(1) Ernst, R. R.; Bodenhausen, G.; Wokaun, A. *Principles of Nuclear Magnetic Resonance in One and Two Dimensions*; Clarendon Press: Oxford, England, 1987.

(2) Tossell, J. A., Ed. *Nuclear Magnetic Shieldings and Molecular Structure*; NATO ASI Series C, Kluwer: Dordrecht, 1993; Vol. 386.
(3) Ditchfield, R. *Mol. Phys.* **1974**, *27*, 789−807.
(4) Wolinski, K.; Hinton, J. F.; Pulay, P. *J. Am. Chem. Soc.* **1990**, *112*, 8251−8260.
(5) Schindler, M.; Kutzelnigg, W. *J. Chem. Phys.* **1982**, *76*, 1919−1933.
(6) Malkin, V. G.; Malkina, O. L.; Casida, M. E.; Salahub, D. R. *J. Am. Chem. Soc.* **1994**, *116*, 5898−5908.
(7) Schreckenbach, G.; Ziegler, T. *J. Phys. Chem.* **1995**, *99*, 606−611.
(8) Frisch, M. J.; Trucks, G. W.; Head-Gordon, M.; Gill, P. M. W.; Wong, M. W.; Foresman, J. B.; Johnson, B. G.; Schlegel, H. B.; Robb, M. A.; Repiogle, E. S.; Gomperts, R.; Andres, J. L.; Raghavachari, K.; Binkley, J. S.; Gonzalez, C.; Martin, R. L.; Fox, D. J.; Defrees, D. J.; Baker, J.; Stewart, J. J. P.; Pople, J. A. Gaussian, Inc.: Pittsburgh, PA, 1994.
(9) Oldfield, E. *J. Biomol. NMR* **1995**, *5*, 217−225.
(10) Oldfield, E.; Keniry, M. A.; Shinoda, S.; Schramm, S.; Brown, T. L.; Gutowsky, H. S. *J. Chem. Soc., Chem. Commun.* **1985**, 791−793.
(11) Kaupp, M.; Malkin, V. G.; Malkina, O. L.; Salahub, D. R. *Chem. Eur. J.* **1996**, *2*, 24−30.
(12) Zilm, K. W.; Conlin, R. T.; Grant, D. M.; Michl, J. *J. Am. Chem. Soc.* **1980**, *102*, 6672−6676.
(13) Zilm, K. W.; Beeler, A. J.; Grant, D. M.; Michl, J.; Chou, T.-C.; Allred, E. L. *J. Am. Chem. Soc.* **1981**, *103*, 2119−2120.
(14) Wallraff, G. M. Thesis, The University of Utah, 1985.
(15) Chatt, J.; Duncanson, L. A. *J. Chem. Soc.* **1953**, 2939−2947.
(16) Dewar, M. J. S. *Colloque international sur les réarrangements moléculaires et l'inversion de Walden*; Montpelier, 1950.
(17) Dewar, M. J. S. *Bull. Soc. Chim. Fr. C* **1951**, *18*, 71−79.
(18) Haight, H. L.; Doyle, J. R.; Baenziger, N. C.; Richards, G. F. *Inorg. Chem.* **1963**, *2*, 1301−1303.
(19) Albinati, A.; Meille, S. V.; Carturan, G. *J. Organomet. Chem.* **1979**, *182*, 269−274.
(20) Kutzelnigg, W.; Fleischer, U.; Schindler, M. in *NMR Basic Principles and Progress*, Springer-Verlag: New York, 1991; Vol. 23, pp 165−262.
(21) Malkin, V. G.; Malkina, O. L., Eriksson, L. A., Salahub, D. R. In *Theoretical and Computational Chemistry*; Politzer, P., Seminario, J. M., Eds.; Elsevier: Amsterdam, 1994; Vol. 1.
(22) Becke, A. D. *J. Chem. Phys.* **1993**, *98*, 5648−5652. Lee, C.; Yang, W.; Parr, R. G. *Phys. Rev. B* **1988**, *37*, 787−789.
(23) Dunning, T. H., Jr., Hay, P. J. In *Modern Theoretical Chemistry*; Plenum: New York, 1976, pp 1−28.
(24) Boeyens, J. C. A.; Denner, L.; Orchard, S. W.; Rencken, I.; Rose, B. G. *S. Afr. J. Chem.* **1986**, *39*, 229−232.
(25) Eller, P. G.; Ryan, R. R.; Schaeffer, R. O. *Cryst. Struct. Commun.* **1977**, *6*, 163−166.
(26) Syed, A.; Stevens, E. D.; Cruz, S. G. *Inorg. Chem.* **1984**, *23*, 3673−3674.
(27) Herzfeld, J.; Berger, A. E. *J. Chem. Phys.* **1980**, *73*, 6021−6030.
(28) Jameson, K. J.; Jameson, C. J. *Chem. Phys. Lett.* **1987**, *134*, 461−466.
(29) Buehl, M. *Chem. Phys. Lett.* **1997**, *267*, 251−257.
(30) Chan, J. C. C.; Au−Yeung, S. C. F. *J. Phys. Chem.* **1997**, *101*, 3637−3640. Godbout, N.; Oldfield, E. *J. Am. Chem. Soc.* In press.
(31) Havlin, R. H.; Godbout, N.; Salzmann, R.; Wojdelski, M.; Arnold, W.; Schulz, C.; Oldfield, E. Unpublished results.
(32) Havlin, R.; Godbout, N.; Oldfield, E. Unpublished results.
(33) Cheeseman, J. R.; Trucks, G. W.; Keith, T. A.; Frisch, M. J. *J. Chem. Phys.* **1996**, *104*, 5497−5509.
(34) Tokuhiro, T.; Fraenkel, G. *J. Am. Chem. Soc.* **1969**, *91*, 5005−5013. Spiesecke, H.; Schneider, W. G. *Tetrahedron Lett.* **1961**, *14*, 468−472.
(35) Jarvis, J. A. J.; Kilbourn, B. T.; Owston, P. G. *Acta Crystallogr., Sect B* **1971**, *27*, 366−372.
(36) Duncan, T. M. *A Compilation of Chemical Shift Anisotropies*; Farragut Press: Chicago, Illinois, 1990.